Extensive functional repertoire underpins complex behaviours: insights from Parkinson's disease

Pierpaolo Sorrentino[1,2,3*], Rosaria Rucco[3,4,5*], Fabio Baselice[1], Rosa De Micco[6], Alessandro Tessitore[6], Arjan Hillebrand[7], Laura Mandolesi[8], Michael Breakspear[9], Leonardo L. Gollo[2+] & Giuseppe Sorrentino[4,5+]

[*] These authors contributed equally to the manuscript

[+] These authors contributed equally to the manuscript

1. University of Naples Parthenope, Department of Engineering, Centro Direzionale, Isola C4, 80143, Naples, Italy
2. QIMR Berghofer, 300 Herston Rd, Brisbane City, QLD 4006, Australia
3. Institute for Applied Science and Intelligent Systems, National Research Council, Via Campi Flegrei 34, Pozzuoli, Italy
4. University of Naples Parthenope, Department of motor sciences and wellness, Via Ammiraglio Ferdinando Acton, 38, 80133, Naples, Italy
5. Hermitage-Capodimonte Hospital, via Cupa delle Tozzole 2, Naples, Italy
6. Department of Advanced Medical and Surgical Sciences, University of Campania "Luigi Vanvitelli", via Luciano Armanni 5, 80138, Naples, Italy
7. Amsterdam UMC, Vrije Universiteit Amsterdam, Department of Clinical Neurophysiology and MEG Center, Amsterdam Neuroscience, De Boelelaan 1117, 1081HV Amsterdam, The Netherlands
8. Department of Humanistic Studies, University of Naples Federico II, via Porta di Massa 1, 80133 Naples, Italy
9. Priority Research Centre for Brain and Mind, The University of Newcastle, Medical Sciences, University Drive, Callaghan NSW 2308, Australia.

Corresponding author: Dr. Pierpaolo Sorrentino. Email: pierpaolo.sorrentino@uniparthenope.it

Abstract

Rapid reconfigurations of brain activity support efficient neuronal communication and flexible behaviour. Suboptimal brain dynamics impair this adaptability, possibly leading to functional deficiencies. We hypothesize that impaired flexibility in brain activity can lead to motor and cognitive symptoms of Parkinson's disease (PD). To test this hypothesis, we studied the 'functional repertoire' – the number of distinct configurations of neural activity – using source-reconstructed magnetoencephalography in PD patients and controls. We found stereotyped brain dynamics and reduced flexibility in PD. The intensity of this reduction was proportional to symptoms severity, and explained by beta-band hyper-synchronization. Moreover, the basal ganglia were prominently involved in the abnormal patterns of brain activity. Our findings support the hypotheses that: symptoms in PD reflect impaired brain flexibility, this impairment preferentially involves the basal ganglia, and beta-band hypersynchronization is associated with reduced brain flexibility. These findings highlight the importance of extensive functional repertoires for behaviour and motor.

Keywords: Parkinson's disease, brain dynamics, functional repertoire, hypersynchronization, magnetoencephalography.

1. Introduction

Brain functioning requires efficient reconfiguration of patterns of activity. This flexibility is essential for the coordinated engagement of brain regions, which underlies complex behaviours. Moreover, dynamic patterns of activity reflect the coordinated engagement of different systems within the brain (Friston et al., 1995; Honey et al., 2007; McIntosh et al., 2008; Tagliazucchi et al., 2014). Accordingly, a large number of distinct patterns of activity ("functional repertoire") indicates flexible dynamics. Growing evidence also indicates that the number of spatio-temporal patterns of activity is maximized at *criticality* (Haldeman and Beggs, 2005). This is a highly variable, adaptive and flexible dynamical regime (Beggs and Plenz, 2004, 2003; Friedman et al., 2012) that optimizes the capability of storing information (Hopfield, 1982), the efficient transmission of information across the brain (Beggs and Plenz, 2003), the response to internal fluctuations (Han et al., 2008; Ji and Wilson, 2007; Luczak et al., 2009; Schulthess et al., 2016) and the detection of external stimuli (Kinouchi and Copelli, 2006; MacLean et al., 2005); for review see (Cocchi et al., 2017).

The study of temporally resolved patterns of activation has recently drawn significant interest (Bassett et al., 2011; Holme and Saramäki, 2012; Pedersen et al., 2017; Zalesky et al., 2014). Furthermore, it has been shown that they may have cognitive and behavioural significance (Shine et al., 2016) . In fact, optimal brain dynamics is necessary in a number of behavioural functions (both motor and cognitive). Brain pathologies might perturb such optimally tuned dynamic regime, shifting the brain to a state where reconfigurations do not occur as efficiently. Hence, the behavioural outcomes that rely on such efficient reconfigurations may be impaired, which may result in specific symptoms. Notably, accounting for temporal variability of brain activity has improved the diagnostic classification of neurodegenerative diseases, suggesting that additional information can indeed be disclosed with such approaches (Carbo et al., 2017; Jie et al., 2018).

Parkinson's disease (PD) is a severe and disabling neurodegenerative disorder. It is characterized by reduced amplitude of movements, and slowing of cognitive processes, imposing major individual and social burden (GBD 2016 Parkinson's Disease Collaborators et al., 2018). The main histopathological finding in PD is a severe nigrostriatal dopamine depletion (Parent and Parent, 2010; Zhang et al., 2015). PD has traditionally been regarded predominantly as a motor disease. However, recent clinical and neuroimaging findings have questioned these views (Weingarten et al., 2015). For example, the first symptoms to appear are often not motor, and the clinical phenotype clearly goes well beyond the motor impairment, with other domains, such as executive functioning, involved (Jankovic, 2008; Zesiewicz et al., 2006). Structural Magnetic Resonance Imaging (MRI) has also confirmed that PD is more widespread than previously thought (Weingarten et al., 2015). Although functional magnetic resonance (fMRI) studies have identified impairment in the corticostriatal network in PD patients, the observed changes in functional connectivity extend into many other brain systems (Filippi et al., 2018). Similarly, magnetoencephalography (MEG) studies have also reported widespread functional connectivity alterations in PD (Cao et al., 2019; Olde Dubbelink et al., 2013; Stoffers et al., 2008; Wiesman et al., 2016) .

Abbreviations:

AAL = Automated Anatomical Labelling; ECG = electrocardiogram; EEG= electroencephalogram; EOG = electrooculogram; fMRI = functional Magnetic Resonance Imaging; Hz = Hertz; ICA= Independent Component Analysis; Ks = Kolmogorov-Smirnov; LCMV = linearly constrained minimum variance; MEG = magnetoencephalography; PCA= Principal Component Analysis; PLM = phase linearity measurement; PD = Parkinson's disease; ROI = region of interest; SVD = singular value decomposition; T=Tesla, UPDRS = Unified Parkinson's disease rating scale.

The brain can be represented as a network, with, at the macro-scale, brain areas as 'nodes' and structural or functional relationships between the brain areas as 'edges' (Rubinov and Sporns, 2010; Sporns et al., 2005), following which the topology of the network can be characterised using graph theory. A rapidly growing body of research now uses graph theory to characterize large-scale patterns of brain activation in health (Bullmore and Sporns, 2009) and disease (Fornito et al., 2013). Graph theory has highlighted the multifaceted nature of large-scale interactions in PD, with studies reporting more-connected networks (Xiao Hu et al., 2015; Xiaofei Hu et al., 2015; Kwak et al., 2010; Sunwoo et al., 2015), less-connected networks (Agosta et al., 2014; Baggio et al., 2015; Bell et al., 2015; Luo et al., 2014; Szewczyk-Krolikowski et al., 2014; Tessitore et al., 2012), and a combination of both (Ma et al., 2015; Manza et al., 2016). However, most research in this area has assumed brain activity to be stationary, and did not explore the structure of dynamic fluctuations in activity.

Recent studies, specifically addressing dynamical changes in PD, demonstrated that patients dwelled in a hyperconnected state more frequently compared to matched controls (Kim et al., 2017), and showed greater network level integration in the medication-OFF compared to the ON state (Shine et al., 2019). These findings suggest that impaired flexibility might be deleterious and potentially also related to clinical symptomatology.

One candidate mechanism of impaired flexibility derives from alterations in excitation and synchronizability (Gollo and Breakspear, 2014; Scarpetta and de Candia, 2013). Optimal flexibility requires a moderate amount of synchronizability (Breakspear, 2002). In contrast, hyper-synchronization can restrict the variability of brain states, entraining the dynamics onto a limited number of patterns. Conversely, too little synchronization also limits the variability of brain states with insufficient integration (Gollo and Breakspear, 2014). This framework may be specifically relevant for PD, where hyperactivation and hypersynchronization (primarily in in the beta band) are linked to clinical disability (Eusebio and Brown, 2009; Hammond et al., 2007; Hutchison et al., 2004). Furthermore, administration of L-DOPA can partly revert aberrant hypersynchronization in the beta band and relieve symptoms (Heinrichs-Graham et al., 2014).

Drawing on this theory, we here hypothesized that functional activity in PD would be less flexible than in matched controls. Moreover, we hypothesized that the basal ganglia would play a particularly important role in determining the occurrence of a reduced number of patterns. Furthermore, we also expected greater symptom expression to be associated with a more restricted dynamic repertoire.

2. Materials and methods

2.1 Cohort description

Consecutive early PD patients, diagnosed according to the diagnostic criteria of the UK Parkinson's Disease Society Brain Bank Diagnostic Criteria (Gibb and Lees, 1988), were recruited at the Movement Disorders Unit of the First Division of Neurology at the University of Campania "Luigi Vanvitelli" (Naples, Italy). Inclusion criteria were: a) PD onset after the age of 40 years, to exclude early onset parkinsonism; b) a modified Hoehn and Yahr (H&Y) stage $\leq$ 2.5. Exclusion criteria were: a) dementia associated with PD according to consensus criteria (Emre et al., 2007); b) relevant cognitive impairment, as evidenced by age- and education-adjusted MoCA score lower than or equal to the Italian cut-off score (Santangelo et al., 2015); c) any other neurological disorder or clinically significant or unstable medical condition (Table 1). Disease severity was assessed using the Hoehn and Yahr (H&Y) stages (Hoehn and Yahr, 1967) and the UPDRS III (Fahn, 1987). Motor clinical assessment was performed in "off-state" (off-medication overnight). Levodopa

equivalent daily dose (LEDD) was calculated for both dopamine agonists (LEDD-DA) and dopamine agonists + L-dopa (total LEDD) (Tomlinson et al., 2010). Global cognition was assessed by means of Montreal Cognitive Assessment (MoCA) (Nasreddine et al., 2005). MoCA consists of 12 subtasks exploring the following cognitive domains: (1) memory (score range 0–5), assessed by means of delayed recall of five nouns, after two verbal presentations; (2) visuospatial abilities (score range 0–4), assessed by a clock-drawing task (3 points) and by copying of a cube (1 point); (3) executive functions (score range 0–4), assessed by means of a brief version of the Trail Making B task (1 point). All participants signed informed consent. The study had local Institutional Human Research Ethics approval and was conducted in accordance to the Declaration of Helsinki (Table 1).

Table 1: Demographic and clinical features of PD patients

	HC (n=38) mean±SD	PD (n=39) mean±SD	p-value
Age	62.05±9.40	64.23±9.36	NS
Sex (M/F)	22/16	23/16	NS
Disease duration (months)	-	33.0±15.4	-
H&Y stage	-	1.8±0.5	-
UPDRS III	-	25.0±9.5	-
MoCA (total)	-	22.4±3.3	-
- Memory	-	1.5±1.5	-
- Visuospatial abilities	-	2.4±1.2	-
- Executive functions	-	2.3±1.4	-
- Attention, concentration and working memory	-	4.9±1.3	-
- Language	-	4.9±1.2	-
- Temporal and spatial orientation	-	5.9±0.4	-
BDI	-	5.2±6.2	-
LEDD total	-	289.9±152.3	-
LEDD DA	-	78.3±129.1	-

Data are given as mean± standard deviation (SD). NS: not significant; PD: Parkinson's disease; HC: healthy controls; H&Y: Hoehn & Yahr; UPDRS: Unified Parkinson's Disease Rating Scale; MoCA: Montreal Cognitive Assessment; BDI: Beck depression inventory; LEDD: Levodopa Equivalent Daily Dose; DA: dopamine-agonist.

2.2 MEG acquisition

Magnetoencephalographic data were acquired in a 163-magnetometers MEG system (Sorrentino et al., 2018), with 9 reference sensors, located in a magnetically shielded room (AtB Biomag UG, Ulm, Germany). The position of four position coils and four reference points (nasion, right and left pre-auricular and apex) were digitized before acquisition, using Fastrak (Polhemus®). MEG data were acquired during two eyes closed resting state segments each 2.5 minutes long. Participants were in off-state, and were requested to relax with eyes closed and not to think of anything in particular. Instructions were delivered immediately prior to each recording via an intercom. Head position was recorded at the start of each recording segment. After an anti-aliasing filter, the data were sampled at 1024 Hz. A 4th-order Butterworth IIR band-pass filter was then applied to remove components below 0.5 and above 48 Hz. The filter was implemented offline using MatLab scripts within the Fieldtrip toolbox 2014 (Oostenveld et al., 2011). Electrocardiogram (ECG) and electrooculogram (EOG) data were also recorded (Gross et al., 2013).

2.3 MRI acquisition

MR images were acquired on a 3-T scanner equipped with an 8-channel parallel head coil (General Electric Healthcare, Milwaukee, WI, USA) either after, or a minimum of 21 days (but not more than one month) before, the MEG recording. Three-dimensional T1-weighted images (gradient-echo sequence Inversion Recovery prepared Fast Spoiled Gradient Recalled-echo, time repetition = 6988 ms, TI = 1100 ms, TE = 3.9 ms, flip angle = 10, voxel size = 1 x 1 x 1.2 mm3) were acquired.

2.4 Preprocessing

A principal component analysis (PCA) was performed to reduce the environmental magnetic noise (Sadasivan P.K. and Narayana Dutt D., 1996). Specifically, the filter was obtained by orthogonalizing the reference signals to obtain a base, projecting the signals from the brain sensors on this noise-base, and subsequently removing these projections in order to obtain clean data (de Cheveigné and Simon, 2007). We adopted the PCA filtering implementation available within the Fieldtrip Toolbox (Oostenveld et al., 2011). The noisy segments of acquisition were identified through visual inspection of the whole dataset by an experienced rater (PS) (Gross et al., 2013). On average, 130 ± 2 channels were used. After that, Independent component analysis (ICA) (Barbati et al., 2004) was also performed to eliminate ECG (typically 1-2 two components) and EOG (0-1 components) contributions to the MEG signals.

2.5 Source reconstruction

Source reconstruction of channel data was performed using a beamforming procedure implemented in the Fieldtrip toolbox (Oostenveld et al., 2011). First, the subject's fiducial points were used to co-register the MEG data to the native subject-specific MRI. Second, using a single shell volume conduction model (Nolte, 2003) and an equivalent current dipole source model, a Linearly Constrained Minimum Variance (LCMV) beamformer (Van Veen et al., 1997), based on the whole pre-processed, broad-band data, was used to reconstruct time series related to the centroids of 116 regions-of-interest (ROIs), derived from the Automated Anatomical Labeling (AAL) atlas (Gong et al., 2009; Hillebrand et al., 2016; Tzourio-Mazoyer et al., 2002). Both the atlas and the MRI were aligned to the head coordinates. We focussed on the first 90 ROIs, excluding those in the cerebellum given the low reliability of the reconstructed signal in this region. For each source, we projected the time series along the dipole direction that explained most variance by means of singular value decomposition (SVD). For each subject, we visually inspected the source-space data to check that no remaining artefact was present at the source-level.

2.6 Analysis of dynamics

2.6.1 Neuronal avalanche and avalanche configuration

To quantify spatio-temporal fluctuations of activity, we first estimated "*Neuronal Avalanches*". To start, each of the 90 source-reconstructed signals were z-transformed (Fig. 4A). Subsequently, each time series was thresholded according to a cut-off of 3 standard deviations (i.e. z =3). The robustness of the results to changes in this threshold were also investigated. We defined a neuronal avalanche as a fluctuation of activity starting when at least one region becomes active ($|z| > 3$) and continuing as long as any region remains active (Fig. 4B).

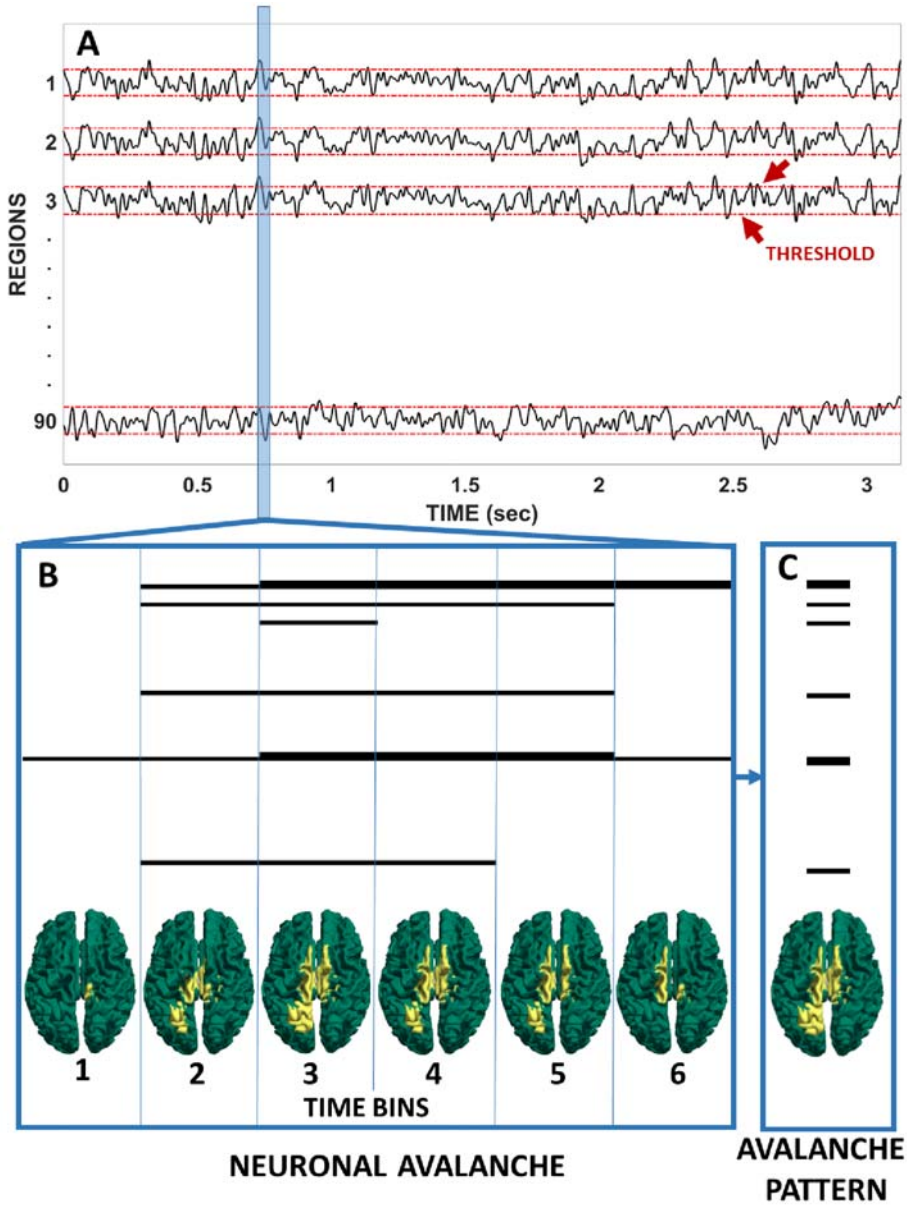

Figure 4. Schematic representation of an avalanche pattern. A. Reconstructed time series (z-scores). The red dashed lines indicate the threshold to define activation. **B.** An avalanche is a sequence of activations that starts when one or more regions are active and ends when no region is active anymore. The brains-plots for each moment (bin) of the avalanche show the active (yellow) and inactive (green) areas C. The areas that were active at some time during the avalanche together form the avalanche pattern.

These analyses require the time series to be binned. To select a suitable bin length, we computed the branching ratio (Haldeman and Beggs, 2005; Harris, 1964), σ, as follows: for each time bin duration, for each subject, for each avalanche, the (geometrically) averaged ratio of the number of events (activations) between the subsequent time bin and that in the current time bin was calculated as,

$$\frac{\quad}{\quad}\frac{\quad}{\quad}\frac{\quad}{\quad}, \qquad (1)$$

where σ_i is the branching parameter of the i-th avalanche in the dataset, N_{bin} is the total number of bins in the i-th avalanche, $n_{events}\ (j)$ is the total number of events in the j-th bin. We then (geometrically) averaged the results over all avalanches (Gollo, 2017),

$$\sigma = \frac{1}{N_{aval}} \prod_{i=1}^{N_{aval}} (\sigma_i)^{\frac{1}{N_{aval}}} \quad , \tag{2}$$

where N_{aval} is the total number of avalanche in each participant's dataset. In branching processes, a branching ratio of σ=1 indicates critical processes with activity that is highly variable and nearly sustained, $\sigma < 1$ indicates subcritical processes in which the activity quickly dies out, and $\sigma > 1$ indicates supercritical processes in which the activity increases. The bin length equal to three yielded a critical process with σ=1, justifying the use of the term "avalanche" for these events. However, the robustness of the results to changes in this exact bin length was also investigated, and the main results were not affected (supplementary material). For each avalanche, an "*avalanche configuration*" was defined as the set of all areas that were active at some point during the avalanche (see Fig. 4C).

2.6.2 Functional repertoire

For each subject, we estimated the functional repertoire, defined as the number of unique avalanche configurations that was expressed during the recording. Before comparing the functional repertoires between groups, the duration of the acquisitions was compared between the two groups, as the acquisition duration could affect the estimate of the functional repertoire. Furthermore, the analysis was also repeated with the (exact) same amount of data for each participant (67.01 seconds). To do so, we selected all participant who had at least a 1 min long acquisition (two patients had less and had to be excluded, leading to 38 controls and 37 patients). We randomly selected data segments from the whole recordings. The results from analysis of these data confirmed our initial analysis (supplementary Fig. 4).

2.6.3 Switching between states

We defined a "switch" as a change of state ("on" to "off" or vice-versa) between two consecutive time – bins, occurring in any area. The switch rate (number of switches over duration), averaged over areas, was computed for each individual.

2.6.4 Analysis of similarity

To estimate and compare the variability of avalanche configurations between groups, we first computed the similarities between each configuration, yielding one distance matrix per group (Haldeman and Beggs, 2005). In each matrix, rows and columns are equal to unique avalanche patterns, while the entries are the Hamming distances (the number of regions that differ- i.e. active or inactive - in two given patterns). Statistical comparison of the similarity matrices belonging to the two groups was achieved by permutation testing (see below for details).

2.6.5 Quantifying the influence of specific regions on avalanche configurations

We split the total functional repertoire in two groups: configurations that occurred in both the clinical and control participants ("shared repertoire"), and configurations that were unique to either group ("group-specific repertoire"). We then computed how often each region occurred in both shared and group-specific configurations. The Kolmogorov – Smirnov test was used to compare the two distributions, and resampling then allowed identification of those regions that appeared in group-specific repertoires more often than by chance.

2.7 Synchrony estimation

To estimate synchronization in the beta band, the broadband source-reconstructed data were band-pass filtered with a fourth order Butterworth filter between 13 and 30 Hz. A metric recently developed by our group (Baselice et al., 2019), the phase linearity measurement (PLM), illustrated in Fig. 5, was then employed to estimate synchronization,

where is the interferometric phase (i.e. the phase of the signal resulting from the multiplication of one signal with the complex conjugate of another signal). The PLM was computed using the implementation available in the Fieldtrip toolbox in Matlab. In short, this metric quantifies the synchronization between two time–series using the central peak in the frequency spectrum of the interferometric signal. The more peaked the spectrum of the interferometric signal, the more the two originating signals will be synchronized. The PLM ranges between 0 and 1, is insensitive to volume conduction and grows monotonically with synchronization (Baselice et al., 2019).

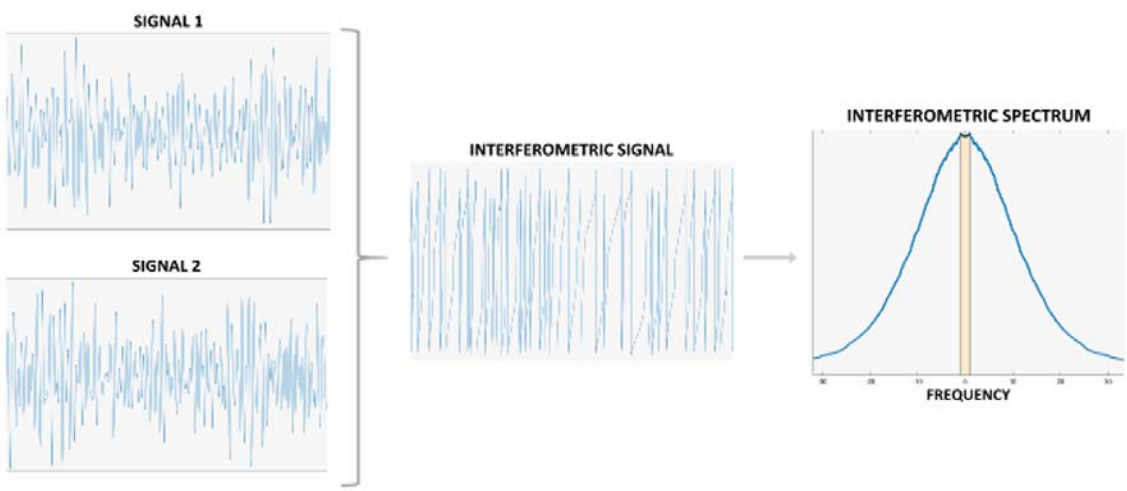

Figure 5. Phase linearity measurement, used to estimate synchronization. The time series of each pair of regions have been processed to obtain the interferometric signal. The power spectrum of the interferometric signal was estimated, and the central area underneath the spectrum (depicted in light brown) was compared to the total area. The higher such ratio, the more synchronized the two signals.

2.8 Statistical analysis

To compare age and sex between the two groups we used T-test and Chi-square test, respectively. Permutation testing (Nichols and Holmes, 2002) or Kolmogorov-Smirnov test were performed to compare patients and controls, as appropriate. For permutation testing, the data where permuted 10000 times, and at each iteration the absolute value of the difference between the two groups was observed, building a null distribution of absolute differences. Finally, the empirical, observed

difference was rank-ordered against this distribution, yielding a significance value. All statistical analyses were performed using custom scripts written in Matlab 2018a.

3. Results

To test these hypotheses, we used source-reconstructed resting state MEG data acquired from a cohort of 39 PD patients and 38 age-matched healthy controls (see Methods for details). We analysed the size of the dynamic repertoire (the number of different unique avalanche configurations, see Methods) and estimated the contribution of individual brain regions to this measure of spontaneous cortical flexibility. Moreover, we correlated the individual flexibility of patients to motor and cognitive outcomes. Finally, we estimated the correlation between synchronization in the beta band and the size of the dynamical repertoire. Data were acquired in two brief segments of eyes-closed resting-state conditions, each of 150 seconds duration. After artefact removal and segment rejection, the average duration of combined recordings was 131.05 seconds in the PD cohort and 131.46 seconds in controls. There was no significant difference in the average recording duration (Wilcoxon rank-sum test, p=0.4539, difference of the average length = 0.41 seconds) or the number of ICA components removed in each group (KS-stats, p = 1.0000 and p = .9999 for electrocardiogram (ECG) and electrooculogram (EOG) components, respectively).We first quantified the functional repertoire of these source-reconstructed resting state MEG data, namely the total number of distinct avalanche configurations within each participant's data. A between-group contrast revealed that PD participants expressed a restricted functional repertoire, visiting a lower number of distinct patterns in comparable amounts of time (permutation test, p=0.0088, see Fig. 1A, B).

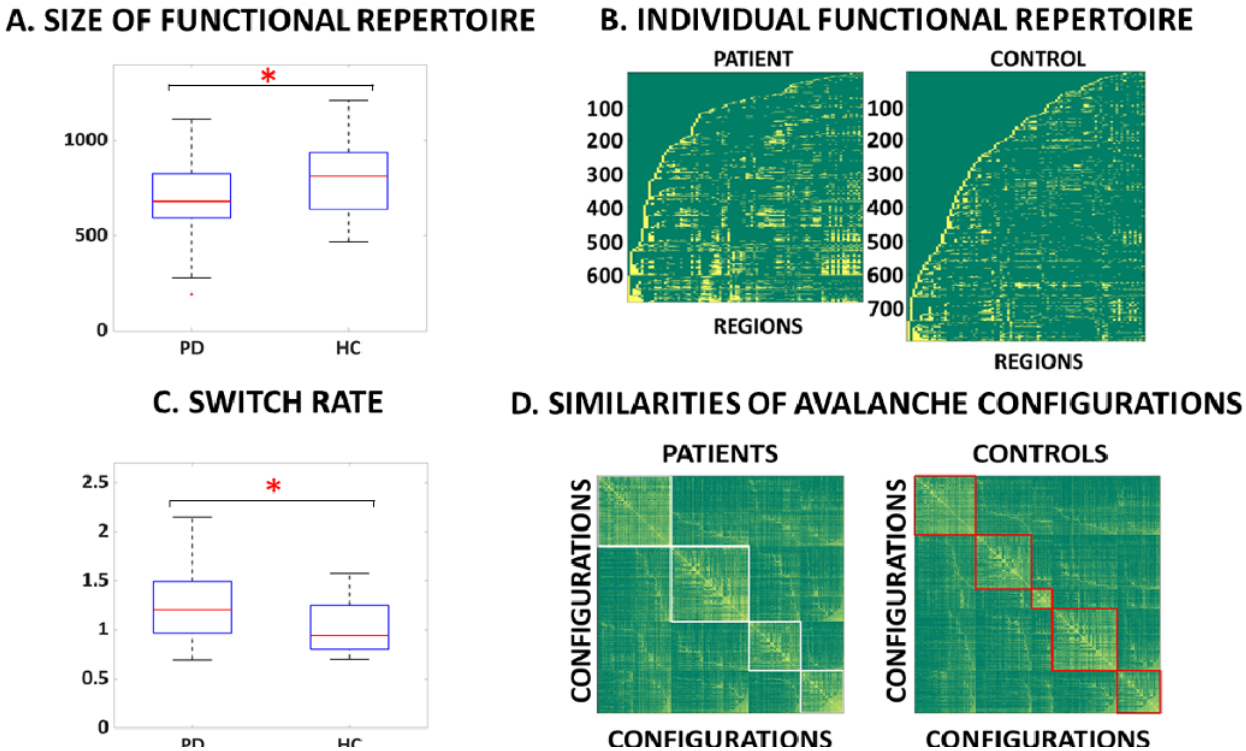

Figure 1. Functional repertoire computed from high spatiotemporal MEG data. A. The number of unique avalanche configurations in PD and healthy controls (HC). The central mark in the box indicates the median, and the edges of the box the 25th and 75th percentiles. The whiskers extend to 3 standard deviations, and the outliers are plotted individually using the '+' symbol. **B.** Avalanche configurations for two representative participants (active regions in yellow, inactive regions in green). On the x-axis, the 90 AAL regions (cortex and basal ganglia). **C.** The number of switches for the two groups. **D.** Boolean similarities between avalanche configurations. Rows and colums show all avalanche configurations that are present in each cohort. The entries are the boolean similarities (i.e. yellow indicates higher similarity). The matrix-entries have been re-ordered using the Louvain modularity algorithm (as implemented in the brain connectivity toolbox), to graphically highlight the presence of clusters. The coloured lines (white and red) show the clusters in patients and controls, respectively.

The size of the functional repertoire correlated negatively with synchronization in the beta band (r = -0.4, *p* = .0070) (Figure 2A). A negative correlation was found between the number of states visited and the clinical severity, as measured by the UPDRS-III, in the PD cohort (r(37) = -0.31, *p* = .026) (Figure 2B).

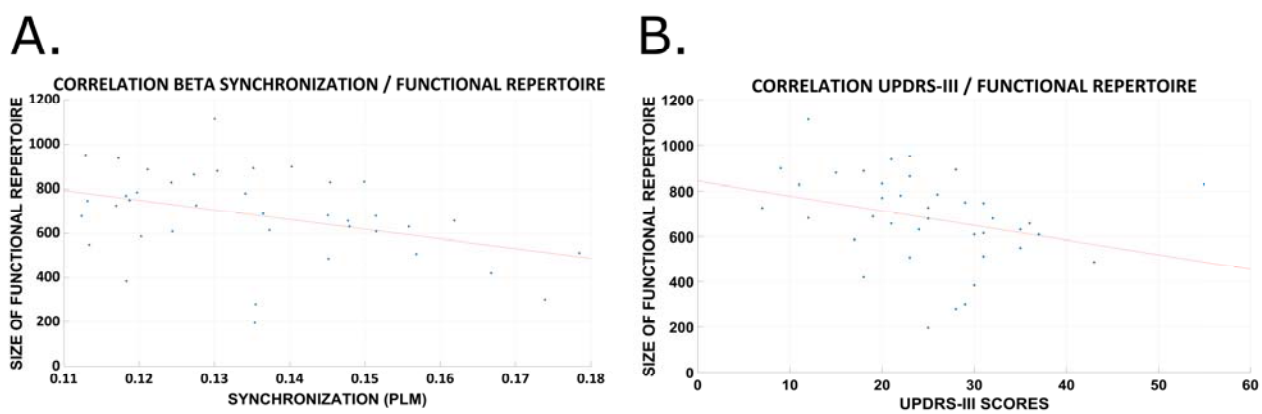

Figure 2. Relationship between flexibility of brain dynamics, clinical disability and global synchronization. A. Correlation between global synchronization, estimated using the phase linearity measurement (PLM) in the beta band, and the size of the functional repertoire.**B.** Correlation between motor impairment, estimated using the Unified Parkinson disease rating scale - III, and the size of the functional repertoire.

When relating the number of visited states with specific cognitive domains, evaluated by the MoCA subscores, linear positive relationships were present with the executive (r(37) = 0.34, *p* = .0352), attention (r(37) = 0.31, *p* = .049), language (r(37) = 0.32, *p* = .044), and naming domains (r(37) = 0.39, *p* = .015). We then compared the switch rate between activated and deactivated states across all areas, capturing the total number of activations regardless of their spatial configuration.

Interestingly, PD patients showed a higher rate of switching (permutation test, p = .0047, Fig. 1C), implying that the decreased diversity of configurations in PD reflected more stereotyped activity, and not fewer activations *per se*.

We moved on to study the heterogeneity of avalanches across members of the same cohort, and compared this heterogeneity between the groups. Permutation testing showed that the Hamming distance across avalanche patterns belonging to either healthy controls or PD differed significantly (permutation testing, p = .0048), where the avalanches in the PD patients were more homogenous in comparison to controls (Fig. 1, D). This finding confirms that the ability to efficiently vary the activation patterns is impaired in PD patients.

Finally, we estimated whether the distribution of the probability of each region to participate in the avalanche patterns differed between those patterns that were specific to a group vs patterns that were present in both groups. Using the Kolmogorov–Smirnov test, we observed that the two distributions were indeed statistically different (p = .012), implying a broad difference between regional involvement in avalanches in each group. Using bootstrapping to perform post-hoc analyses, we identified those regions that appeared more frequently in avalanche patterns that were unique to one group. The pallidum bilaterally (p = 0.03, p = 0.02, left and right, respectively), the left thalamus (p = 0.03), and the right putamen (p = 0.04) were more often involved in avalanches in the PD group than in the controls. Furthermore, the caudate bilaterally, the right thalamus and the left putamen showed differences that did not reach statistical significance (see Fig. 3).

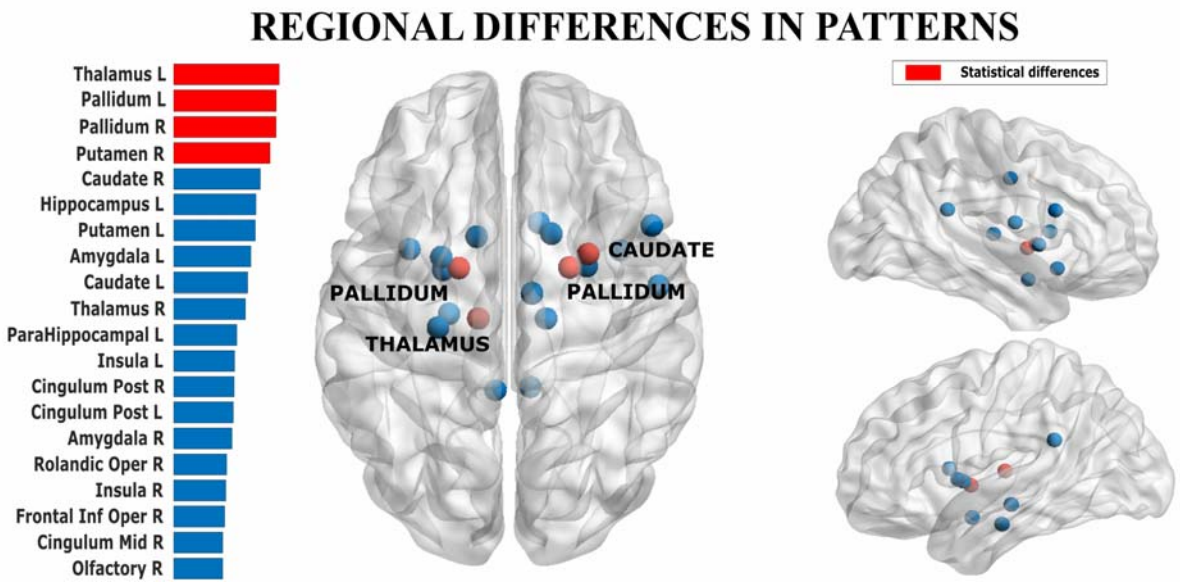

Figure 3. Mapping regional contribution to functional repertoire. The regions that contributed most often to avalanche patterns that were unique to one group. In the bar plot on the left, the width of the bar corresponds to the group difference in frequency with which a region contributed to the avalanche patterns that were unique to a group.

We tested the robustness of our results to specific choices of the avalanche threshold and bin length by varying these variables across a moderate range of values and repeating the analyses. Specifically, we first used different binnings, ranging from 1 to 5 (i.e. time points of the binarized time series were grouped according to the different binnings). The results remained unchanged, with patients displaying a restricted functional repertoire for all binnings explored (for the case of

no binning (binning=1) and binning equal to 5, p = 0.011 and p = 0.0068, respectively; see supplementary Fig.1). Furthermore, the avalanche threshold was modified, ranging from 2.5 to 3.5. For both cases the differences between the groups were confirmed (for z=2.5 and 3.5, p = 0.0084 and p = 0.0082, respectively; see supplementary Fig. 2). We also studied the impact of including cerebellar sources, and the difference in functional repertoire remained significant (p = 0.0042; see supplementary Fig. 3). The analysis was also repeated for the classical frequency bands (i.e. delta, 0.4 – 4 Hz, theta 4 – 8 Hz, alpha 8 – 13 Hz, beta 13- 30 Hz, gamma 30 – 48 Hz). In all the frequency bands, the difference in functional repertoire remained significant (p = 0.049, p = 0.020, p = 0.0065, p = 0.028, p = 0.026, from delta to gamma, respectively; supplementary Fig. 3). These results suggest that the restriction of the functional repertoire in PD is a widespread phenomenon in terms of the range of frequencies involved. Finally, when repeating the analysis using the exact same amount of data for all subjects, the group difference in functional repertoire remained significant (p<0.0001, for broadband; see supplementary Fig. 4).

4. Discussion

Here we investigated time-resolved flexibility of brain activity in PD, utilizing avalanches and tools from statistical physics, adapted to MEG activity. The functional repertoire was formed by distinct patterns of activation during avalanches, and the size of the functional repertoire was used as an indicator of the ease of transitions between different brain states, and hence cognitive flexibility (Cocchi et al., 2017). We found that PD patients exhibited a reduced functional repertoire compared to healthy controls. Moreover, the clinical disability was more pronounced in patients whose functional repertoire was more impoverished. Finally, we demonstrated the robustness of our results across a range of parameters and frequency bands, showing that the results did not depend on specific details of data processing.

Our results showed that PD patients display a restricted functional repertoire as compared to healthy controls. This was demonstrated by the lower number of distinct avalanche configurations. We focused on the flexibility of the brain activity, since efficient reconfiguration of active areas, avoids stereotyped, repetitive dynamics, and has been shown to be important for optimal brain functioning (Grady and Garrett, 2018; McIntosh et al., 2008; Park et al., 2011; Zalesky et al., 2014). The qualitative restriction in the number of patterns of activation explored by PD patients reflects the effect of pathophysiological changes on the large-scale brain dynamics. A recent EEG study that addressed large-scale dynamics found that the duration, rather than the specific order, of functional states related with symptomatology in patients with Lewy body dementia (Schumacher et al., 2019), which is a disease that shows clinical and pathological similarities to PD (Spillantini et al., 1998). However, the same relationship could not be found in PD patients (Schumacher et al., 2019). Our results add to these findings, indicating that the functional repertoire itself is relevant in PD and related to the clinical picture. In our study, we also tested if the restricted functional repertoire was a result of a slower rate of change of state (i.e. between active or inactive) of each region. Interestingly, we found a higher switching rate in PD compared to the healthy controls, suggesting that the restriction of the functional repertoire in PD is qualitative in nature, and not due to a slowing of the regional rate of changes between active and inactive states. The length of the analyzed time series did not differ significantly between the two groups, thus this result could not be explained by the duration of the acquisitions. Importantly, our results replicated when frequency–specific signals were analysed, showing that the slowing of activity that is normally seen in PD also cannot explain the observed differences in the size of the functional repertoire.

We analyzed shared and group-specific avalanche patterns. We classified any pattern as ‘shared’ if it occurred in both groups, and as ‘group-specific’ if it occurred in either group, in order to test whether some regions are specifically important in defining pathological activity patterns. The basal

ganglia belonged to group-specific patterns more often than expected by chance, suggesting that the network of regions that is dynamically connected with the basal ganglia is altered in Parkinson's disease. This finding highlights the importance of a network perspective on brain activity, whereby the basal ganglia show their role in defining the whole-brain dynamical repertoire. This evidence speaks to a vast literature on the basal ganglia as part of a distributed forebrain network with a prominent role in innate behavioral routines as well as learning (retrieving) new (previously acquired) functional repertoires (Graybiel, 1995; Mink, 1996; Wei et al., 2015). Previous evidence has shown that extreme specificity is necessary in the connections between the basal ganglia, thalamus and cortex (Cowan and Wilson, 1994; Flaherty and Graybiel, 1994; Parthasarathy et al., 1992), and that the basal ganglia play a prominent role in the fine tuning of such connections (Forstmann et al., 2008). Our results suggest that the functional role of the basal ganglia might contribute to appropriate dynamical recruitment selection of brain regions.

Importantly, we tested if the restriction of the functional repertoire related to behavioral outcomes. In fact, according to our hypothesis, we expect that impaired brain dynamics at rest would underpin reduce capability to accomplish to a variety of complex tasks. The Unified Parkinson's disease rating scale-III (UPDRS-III) is widely used to assess PD patients, and it provides a quick account of motor symptoms severity in PD. In line with our hypothesis, an inverse relationship was evident between the restriction of the functional repertoire and the UPDRS-III. This evidence supports the interpretation of the restricted functional repertoire as pathological, and points towards the idea that an impaired regulation of the brain dynamics by the basal ganglia underlies clinical impairment in PD. In the same line of thinking, the positive correlations that were present between performance on specific cognitive domains and the size of the functional repertoire, confirms that flexible activity is important for performance on a number of behavioral tasks, not limited to the motor domain. Finally, these result highlight the importance of future longitudinal studies to test the performance of the size of the functional repertoire as a potential biomarker of disease progression.

With regard to the mechanisms underpinning the lack of flexibility, these might involve perturbations in the ability to synchronize different areas (Gollo and Breakspear, 2014). Since PD has often been associated with excessive synchronization (Park et al., 2011), we expected to find a reduction in the size of functional repertoire for patients with a more pronounced hypersynchronization in the beta band, which is classically involved in PD (Heinrichs-Graham et al., 2014). Our results confirmed this predicted negative relation between the number of different patterns of activation and the overall synchronization in the beta band.

Electrophysiological studies in animal models of PD (Bergman et al., 1998; Hammond et al., 2007; Stewart and Plenz, 2006) and in patients with PD have shown that dopaminergic depletion can increase oscillatory activity in the thalamo-cortical circuitry. Furthermore, while this activity has been described in multiple frequency bands, the beta band is specifically relevant to PD (Heinrichs-Graham et al., 2014). The extent of such aberrant beta synchronization has been related to clinical disability, and L-DOPA has been shown to partly revert this phenomenon and relieve symptoms (Heinrichs-Graham et al., 2014). Accordingly, EEG data from PD patients showed that the lack of dopamine increases coupling strength in the basal ganglia circuitry (Park et al., 2011). Within this framework, our results indicate that a hypersynchronized state is deleterious as it reduces the flexibility of brain activity. In fact, excessive synchronization reduces the variability of the behaviour of the system, hence narrowing the number of states that are readily accessible (Gollo and Breakspear, 2014; Pikovsky et al., 2003; Yang et al., 2012). Hypersynchronization and hyperconnected topology have been associated with a variety of neurological diseases (Rucco et al., 2019; Sorrentino et al., 2018), as well as in preclinical conditions that carry an increased risk of neurodegeneration (Sorrentino et al., 2017) hence investigations of the functional repertoires in these diseases and conditions could provide answers to this question.

Some limitations of our work should be considered when interpreting our results. First, we utilised the automated anatomicl labelling (AAL) atlas when reconstructing the neuronal activity, which is well suited to MEG studies but has a somewhat coarse spatial resolution. Taking into account that this work is based on MEG signals, it is important to consider that more fine-grained atlases might go over the nominal resolution of the source-reconstructed signal, which could lead to spurious results. Interestingly, parcellations that are based on MEG resting state data contain roughly the same number of parcels as the AAL atlas (Farahibozorg et al., 2018). Hence, we believe that this choice of atlas yields a reasonable compromise between obtaining high spatio-temporal resolution while avoiding an overestimation of the coactivations that might be induced by atlas with a too high spatial resolution. Furthermore, we chose to focus our main analysis on 90 regions, excluding the cerebellum, as the parcellation of the cerebellum in the AAL atlas is particularly fine grained, the posterior fossa is prone to artefact, and MEG does not provide high spatial resolution. However, the role of the cerebellum is undoubtedly important in PD (O'Callaghan et al., 2016). For this reason, we also repeated the analysis with all 116 AAL regions, including the cerebellum. All the significant group differences were confirmed, proving the robustness of the findings. Furthermore, we chose to include the basal ganglia in the analysis, given the paramount importance of their role in PD. Nonetheless, it is worth to consider that the sensitivity of MEG (Hillebrand and Barnes, 2002), and thereby the quality of the source reconstruction, tends to decay with the depth of the analysed brain structure. Hence, the analysis involving the basal ganglia is based on a reconstructed signal that may have suboptimal resolution (as compared to the cortical data).However, it has recently been shown that magnetoencephalography can indeed detect the activity of deep brain sources (Hillebrand et al., 2016; Meyer et al., 2017; Pizzo et al., 2019).

In conclusion, our results show that a more stereotyped brain activity impairs the ability of the brain to perform complex tasks and is related to hypersynchronization. Furthermore, we show that most of the symptoms that characterize PD can be explained within this framework. In fact, our results show that the brain of PD patients is less flexible. Crucially, the size of the functional repertoire is proportional to the observed clinical disability. The known role the basal ganglia play in defining PD pathophysiology naturally emerges within this framework, in their marked involvement in pathological configurations. Our findings also indicate that the mechanisms underlying impaired flexibility of brain activity relates with the observed clinical phenotype observed in PD, and to hypersynchronization. This also provides a new interpretation of PD pathophysiology in which the well-known beta hypersynchronization is associated with suboptimal brain dynamics.

Data availability

The MEG data and the reconstructed avalanches are available upon reasonable request to the corresponding author, conditional on appropriate ethics approval at the local site.

Funding

This study was funded by University of Naples Parthenope within the Project "Bando Ricerca Competitiva 2017" (D.R. 289/2017). LLG is funded by NHMRC-ARC fellowship ID: APP1110975.

References

Agosta, F., Caso, F., Stankovic, I., Inuggi, A., Petrovic, I., Svetel, M., Kostic, V.S., Filippi, M., 2014. Cortico-striatal-thalamic network functional connectivity in hemiparkinsonism. Neurobiol. Aging 35, 2592–2602. https://doi.org/10.1016/j.neurobiolaging.2014.05.032

Baggio, H.C., Segura, B., Garrido-Millan, J.L., Marti, M.-J., Compta, Y., Valldeoriola, F., Tolosa, E., Junque, C., 2015. Resting-state frontostriatal functional connectivity in Parkinson's disease-related apathy. Mov. Disord. 30, 671–9. https://doi.org/10.1002/mds.26137

Barbati, G., Porcaro, C., Zappasodi, F., Rossini, P.M., Tecchio, F., 2004. Optimization of an independent component analysis approach for artifact identification and removal in magnetoencephalographic signals. Clin. Neurophysiol. 115, 1220–1232. https://doi.org/10.1016/j.clinph.2003.12.015

Baselice, F., Sorriso, A., Rucco, R., Sorrentino, P., 2019. Phase Linearity Measurement: A Novel Index for Brain Functional Connectivity. IEEE Trans. Med. Imaging 38, 873–882. https://doi.org/10.1109/TMI.2018.2873423

Bassett, D.S., Wymbs, N.F., Porter, M.A., Mucha, P.J., Carlson, J.M., Grafton, S.T., 2011. Dynamic reconfiguration of human brain networks during learning. Proc. Natl. Acad. Sci. 108, 7641–7646. https://doi.org/10.1073/pnas.1018985108

Beggs, J.M., Plenz, D., 2004. Neuronal Avalanches Are Diverse and Precise Activity Patterns That Are Stable for Many Hours in Cortical Slice Cultures. J. Neurosci. 24, 5216–5229. https://doi.org/10.1523/JNEUROSCI.0540-04.2004

Beggs, J.M., Plenz, D., 2003. Neuronal avalanches in neocortical circuits. J. Neurosci. 23, 11167–77.

Bell, P.T., Gilat, M., O'Callaghan, C., Copland, D.A., Frank, M.J., Lewis, S.J.G., Shine, J.M., 2015. Dopaminergic basis for impairments in functional connectivity across subdivisions of the striatum in Parkinson's disease. Hum. Brain Mapp. 36, 1278–1291. https://doi.org/10.1002/hbm.22701

Bergman, H., Feingold, A., Nini, A., Raz, A., Slovin, H., Abeles, M., Vaadia, E., 1998. Physiological aspects of information processing in the basal ganglia of normal and parkinsonian primates. Trends Neurosci. 21, 32–8.

Breakspear, M., 2002. Nonlinear phase desynchronization in human electroencephalographic data. Hum. Brain Mapp. 15, 175–198. https://doi.org/10.1002/hbm.10011

Bullmore, E., Sporns, O., 2009. Complex brain networks: graph theoretical analysis of structural and functional systems. Nat. Rev. Neurosci. 10, 186–198. https://doi.org/10.1038/nrn2575

Cao, C., Li, D., Zeng, K., Zhan, S., Huang, P., Li, X., Sun, B., 2019. Levodopa Reduces the Phase lag Index of Parkinson's Disease Patients: A Magnetoencephalographic Study. Clin. EEG Neurosci. 50, 134–140. https://doi.org/10.1177/1550059418781693

Carbo, E.W.S., Hillebrand, A., van Dellen, E., Tewarie, P., de Witt Hamer, P.C., Baayen, J.C., Klein, M., Geurts, J.J.G., Reijneveld, J.C., Stam, C.J., Douw, L., 2017. Dynamic hub load predicts cognitive decline after resective neurosurgery. Sci. Rep. 7, 42117. https://doi.org/10.1038/srep42117

Cocchi, L., Gollo, L.L., Zalesky, A., Breakspear, M., 2017. Criticality in the brain: A synthesis of neurobiology, models and cognition. Prog. Neurobiol. 158, 132–152. https://doi.org/10.1016/J.PNEUROBIO.2017.07.002

Cowan, R.L., Wilson, C.J., 1994. Spontaneous firing patterns and axonal projections of single corticostriatal neurons in the rat medial agranular cortex. J. Neurophysiol. 71, 17–32. https://doi.org/10.1152/jn.1994.71.1.17

de Cheveigné, A., Simon, J.Z., 2007. Denoising based on time-shift PCA. J. Neurosci. Methods 165, 297–305. https://doi.org/10.1016/J.JNEUMETH.2007.06.003

Emre, M., Aarsland, D., Brown, R., Burn, D.J., Duyckaerts, C., Mizuno, Y., Broe, G.A., Cummings, J., Dickson, D.W., Gauthier, S., Goldman, J., Goetz, C., Korczyn, A., Lees, A., Levy, R., Litvan, I., McKeith, I., Olanow, W., Poewe, W., Quinn, N., Sampaio, C., Tolosa, E., Dubois, B., 2007. Clinical diagnostic criteria for dementia associated with Parkinson's disease. Mov. Disord. 22, 1689–1707. https://doi.org/10.1002/mds.21507

Eusebio, A., Brown, P., 2009. Synchronisation in the beta frequency-band — The bad boy of parkinsonism or an innocent bystander? Exp. Neurol. 217, 1–3. https://doi.org/10.1016/j.expneurol.2009.02.003

Fahn, S., 1987. Unified Parkinson's Disease Rating Scale. Recent Dev. Park. Dis.

Farahibozorg, S.-R., Henson, R.N., Hauk, O., 2018. Adaptive cortical parcellations for source reconstructed EEG/MEG connectomes. Neuroimage 169, 23–45. https://doi.org/10.1016/J.NEUROIMAGE.2017.09.009

Filippi, M., Elisabetta, S., Piramide, N., Agosta, F., 2018. Functional MRI in Idiopathic Parkinson's Disease. Int. Rev. Neurobiol. 141, 439–467. https://doi.org/10.1016/BS.IRN.2018.08.005

Flaherty, A., Graybiel, A., 1994. Input-output organization of the sensorimotor striatum in the squirrel monkey. J Neurosci. 14, 599–610.

Fornito, A., Zalesky, A., Breakspear, M., 2013. Graph analysis of the human connectome: Promise, progress, and pitfalls. Neuroimage 80, 426–444. https://doi.org/10.1016/j.neuroimage.2013.04.087

Forstmann, B.U., Dutilh, G., Brown, S., Neumann, J., von Cramon, D.Y., Ridderinkhof, K.R., Wagenmakers, E.-J., 2008. Striatum and pre-SMA facilitate decision-making under time pressure. Proc. Natl. Acad. Sci. U. S. A. 105, 17538–42. https://doi.org/10.1073/pnas.0805903105

Friedman, N., Ito, S., Brinkman, B.A.W., Shimono, M., DeVille, R.E.L., Dahmen, K.A., Beggs, J.M., Butler, T.C., 2012. Universal critical dynamics in high resolution neuronal avalanche data. Phys. Rev. Lett. 108, 208102. https://doi.org/10.1103/PhysRevLett.108.208102

Friston, K.J., Tononi, G., Sporns, O., Edelman, G.M., 1995. Characterising the complexity of neuronal interactions. Hum. Brain Mapp. 3, 302–314. https://doi.org/10.1002/hbm.460030405

GBD 2016 Parkinson's Disease Collaborators, E.R., Elbaz, A., Nichols, E., Abd-Allah, F., Abdelalim, A., Adsuar, J.C., Ansha, M.G., Brayne, C., Choi, J.-Y.J., Collado-Mateo, D., Dahodwala, N., Do, H.P., Edessa, D., Endres, M., Fereshtehnejad, S.-M., Foreman, K.J., Gankpe, F.G., Gupta, R., Hankey, G.J., Hay, S.I., Hegazy, M.I., Hibstu, D.T., Kasaeian, A., Khader, Y., Khalil, I., Khang, Y.-H., Kim, Y.J., Kokubo, Y., Logroscino, G., Massano, J., Ibrahim, N.M., Mohammed, M.A., Mohammadi, A., Moradi-Lakeh, M., Naghavi, M., Nguyen, B.T., Nirayo, Y.L., Ogbo, F.A., Owolabi, M.O., Pereira, D.M., Postma, M.J., Qorbani, M., Rahman, M.A., Roba, K.T., Safari, H., Safiri, S., Satpathy, M., Sawhney, M., Shafieesabet, A., Shiferaw, M.S., Smith, M., Szoeke, C.E.I., Tabarés-Seisdedos, R., Truong, N.T., Ukwaja, K.N., Venketasubramanian, N., Villafaina, S., weldegwergs, K. gidey, Westerman, R., Wijeratne, T., Winkler, A.S., Xuan, B.T., Yonemoto, N., Feigin, V.L., Vos, T., Murray, C.J.L., 2018. Global, regional, and national burden of Parkinson's disease, 1990-2016: a systematic analysis for the Global Burden of Disease Study 2016. Lancet. Neurol. 17, 939–953. https://doi.org/10.1016/S1474-4422(18)30295-3

Gibb, W.R., Lees, A.J., 1988. A comparison of clinical and pathological features of young- and old-onset Parkinson's disease. Neurology 38, 1402–6. https://doi.org/10.1212/wnl.38.9.1402

Gollo, L.L., 2017. Coexistence of critical sensitivity and subcritical specificity can yield optimal population coding. J. R. Soc. Interface 14. https://doi.org/10.1098/rsif.2017.0207

Gollo, L.L., Breakspear, M., 2014. The frustrated brain: from dynamics on motifs to communities and networks. Philos. Trans. R. Soc. B Biol. Sci. 369, 20130532–20130532. https://doi.org/10.1098/rstb.2013.0532

Gong, G., He, Y., Concha, L., Lebel, C., Gross, D.W., Evans, A.C., Beaulieu, C., 2009. Mapping anatomical connectivity patterns of human cerebral cortex using in vivo diffusion tensor imaging tractography. Cereb. Cortex 19, 524–36. https://doi.org/10.1093/cercor/bhn102

Grady, C.L., Garrett, D.D., 2018. Brain signal variability is modulated as a function of internal and external demand in younger and older adults. Neuroimage 169, 510–523. https://doi.org/10.1016/j.neuroimage.2017.12.031

Graybiel, A.M., 1995. Building action repertoires: memory and learning functions of the basal ganglia. Curr. Opin. Neurobiol. 5, 733–41.

Gross, J., Baillet, S., Barnes, G.R., Henson, R.N., Hillebrand, A., Jensen, O., Jerbi, K., Litvak, V., Maess, B., Oostenveld, R., Parkkonen, L., Taylor, J.R., van Wassenhove, V., Wibral, M., Schoffelen, J.-M., 2013. Good practice for conducting and reporting MEG research. Neuroimage 65, 349–63. https://doi.org/10.1016/j.neuroimage.2012.10.001

Haldeman, C., Beggs, J.M., 2005. Critical Branching Captures Activity in Living Neural Networks and Maximizes the Number of Metastable States. Phys. Rev. Lett. 94, 058101. https://doi.org/10.1103/PhysRevLett.94.058101

Hammond, C., Bergman, H., Brown, P., 2007. Pathological synchronization in Parkinson's disease: networks, models and treatments. Trends Neurosci. 30, 357–64. https://doi.org/10.1016/j.tins.2007.05.004

Han, F., Caporale, N., Dan, Y., 2008. Reverberation of Recent Visual Experience in Spontaneous Cortical Waves. Neuron 60, 321–327. https://doi.org/10.1016/j.neuron.2008.08.026

Harris, T.E., 1964. The Theory of Branching Process.

Heinrichs-Graham, E., Kurz, M.J., Becker, K.M., Santamaria, P.M., Gendelman, H.E., Wilson, T.W., 2014. Hypersynchrony despite pathologically reduced beta oscillations in patients with Parkinson's disease: a

pharmaco-magnetoencephalography study. J. Neurophysiol. 112.

Hillebrand, A., Barnes, G.R., 2002. A quantitative assessment of the sensitivity of whole-head MEG to activity in the adult human cortex. Neuroimage 16, 638–50.

Hillebrand, A., Nissen, I.A., Ris-Hilgersom, I., Sijsma, N.C.G., Ronner, H.E., van Dijk, B.W., Stam, C.J., 2016. Detecting epileptiform activity from deeper brain regions in spatially filtered MEG data. Clin. Neurophysiol. 127, 2766–2769. https://doi.org/10.1016/j.clinph.2016.05.272

Hoehn, M.M., Yahr, M.D., 1967. Parkinsonism: onset, progression, and mortality. Neurology 17, 427–427. https://doi.org/10.1212/WNL.17.5.427

Holme, P., Saramäki, J., 2012. Temporal networks. Phys. Rep. 519, 97–125. https://doi.org/10.1016/J.PHYSREP.2012.03.001

Honey, C.J., Kötter, R., Breakspear, M., Sporns, O., 2007. Network structure of cerebral cortex shapes functional connectivity on multiple time scales. Proc. Natl. Acad. Sci. U. S. A. 104, 10240–5. https://doi.org/10.1073/pnas.0701519104

Hopfield, J.J., 1982. Neural networks and physical systems with emergent collective computational abilities. Proc. Natl. Acad. Sci. U. S. A. 79, 2554–8.

Hu, Xiao, Song, X., Li, E., Liu, J., Yuan, Y., Liu, W., Liu, Y., 2015. Altered Resting-State Brain Activity and Connectivity in Depressed Parkinson's Disease. PLoS One 10, e0131133. https://doi.org/10.1371/journal.pone.0131133

Hu, Xiaofei, Zhang, J., Jiang, X., Zhou, C., Wei, L., Yin, X., Wu, Y., Li, J., Zhang, Y., Wang, J., 2015. Decreased interhemispheric functional connectivity in subtypes of Parkinson's disease. J. Neurol. 262, 760–7. https://doi.org/10.1007/s00415-014-7627-x

Hutchison, W.D., Dostrovsky, J.O., Walters, J.R., Courtemanche, R., Boraud, T., Goldberg, J., Brown, P., 2004. Annual Meeting Mini-Symposium Neuronal Oscillations in the Basal Ganglia and Movement Disorders: Evidence from Whole Animal and Human Recordings. https://doi.org/10.1523/JNEUROSCI.3366-04.2004

Jankovic, J., 2008. Parkinson's disease clinical features and diagnosis. J Neurol Neurosurg Psychiatry 79, 368–376. https://doi.org/http://dx.doi.org/10.1136/jnnp.2007.131045

Ji, D., Wilson, M.A., 2007. Coordinated memory replay in the visual cortex and hippocampus during sleep. Nat. Neurosci. 10, 100–7. https://doi.org/10.1038/nn1825

Jie, B., Liu, M., Shen, D., 2018. Integration of temporal and spatial properties of dynamic connectivity networks for automatic diagnosis of brain disease. Med. Image Anal. 47, 81–94. https://doi.org/10.1016/j.media.2018.03.013

Kim, J., Criaud, M., Cho, S.S., Díez-Cirarda, M., Mihaescu, A., Coakeley, S., Ghadery, C., Valli, M., Jacobs, M.F., Houle, S., Strafella, A.P., 2017. Abnormal intrinsic brain functional network dynamics in Parkinson's disease. Brain 140, 2955–2967. https://doi.org/10.1093/brain/awx233

Kinouchi, O., Copelli, M., 2006. Optimal dynamical range of excitable networks at criticality. Nat. Phys. 2, 348–351. https://doi.org/10.1038/nphys289

Kwak, Y., Peltier, S., Bohnen, N.I., Müller, M.L.T.M., Dayalu, P., Seidler, R.D., 2010. Altered resting state cortico-striatal connectivity in mild to moderate stage Parkinson's disease. Front. Syst. Neurosci. 4, 143. https://doi.org/10.3389/fnsys.2010.00143

Luczak, A., Barthó, P., Harris, K.D., 2009. Spontaneous events outline the realm of possible sensory responses in neocortical populations. Neuron 62, 413–25. https://doi.org/10.1016/j.neuron.2009.03.014

Luo, C., Chen, Q., Song, W., Chen, K., Guo, X., Yang, J., Huang, X., Gong, Q., Shang, H.-F., 2014. Resting-state fMRI study on drug-naive patients with Parkinson's disease and with depression. J. Neurol. Neurosurg. Psychiatry 85, 675–83. https://doi.org/10.1136/jnnp-2013-306237

Ma, H., Chen, H., Fang, J., Gao, L., Ma, L., Wu, T., Hou, Y., Zhang, J., Feng, T., 2015. Resting-state functional connectivity of dentate nucleus is associated with tremor in Parkinson's disease. J. Neurol. 262, 2247–56. https://doi.org/10.1007/s00415-015-7835-z

MacLean, J.N., Watson, B.O., Aaron, G.B., Yuste, R., 2005. Internal Dynamics Determine the Cortical Response to Thalamic Stimulation. Neuron 48, 811–823. https://doi.org/10.1016/j.neuron.2005.09.035

Manza, P., Zhang, S., Li, C.-S.R., Leung, H.-C., 2016. Resting-state functional connectivity of the striatum in early-stage Parkinson's disease: Cognitive decline and motor symptomatology. Hum. Brain Mapp. 37, 648–662. https://doi.org/10.1002/hbm.23056

McIntosh, A.R., Kovacevic, N., Itier, R.J., 2008. Increased Brain Signal Variability Accompanies Lower Behavioral Variability in Development. PLoS Comput. Biol. 4, e1000106. https://doi.org/10.1371/journal.pcbi.1000106

Meyer, S.S., Rossiter, H., Brookes, M.J., Woolrich, M.W., Bestmann, S., Barnes, G.R., 2017. Using generative models to make probabilistic statements about hippocampal engagement in MEG. Neuroimage 149, 468–482. https://doi.org/10.1016/J.NEUROIMAGE.2017.01.029

Mink, J.W., 1996. The basal ganglia: focused selection and inhibition of competing motor programs. Prog. Neurobiol. 50, 381–425.

Nasreddine, Z.S., Phillips, N.A., BÃ©dirian, V., Charbonneau, S., Whitehead, V., Collin, I., Cummings, J.L., Chertkow, H., 2005. The Montreal Cognitive Assessment, MoCA: A Brief Screening Tool For Mild Cognitive Impairment. J. Am. Geriatr. Soc. 53, 695–699. https://doi.org/10.1111/j.1532-5415.2005.53221.x

Nichols, T.E., Holmes, A.P., 2002. Nonparametric permutation tests for functional neuroimaging: a primer with examples. Hum. Brain Mapp. 15, 1–25.

Nolte, G., 2003. The magnetic lead field theorem in the quasi-static approximation and its use for magnetoencephalography forward calculation in realistic volume conductors. Phys. Med. Biol. 48, 3637–3652. https://doi.org/10.1088/0031-9155/48/22/002

O'Callaghan, C., Hornberger, M., Balsters, J.H., Halliday, G.M., Lewis, S.J.G., Shine, J.M., 2016. Cerebellar atrophy in Parkinson's disease and its implication for network connectivity. Brain 139, 845–855. https://doi.org/10.1093/brain/awv399

Olde Dubbelink, K.T.E., Stoffers, D., Deijen, J.B., Twisk, J.W.R., Stam, C.J., Hillebrand, A., Berendse, H.W., 2013. Resting-state functional connectivity as a marker of disease progression in Parkinson's disease: A longitudinal MEG study. NeuroImage Clin. 2, 612–619. https://doi.org/10.1016/J.NICL.2013.04.003

Oostenveld, R., Fries, P., Maris, E., Schoffelen, J.-M., 2011. FieldTrip: Open source software for advanced analysis of MEG, EEG, and invasive electrophysiological data. Comput. Intell. Neurosci. 2011, 156869. https://doi.org/10.1155/2011/156869

Parent, M., Parent, A., 2010. Substantia nigra and Parkinson's disease: a brief history of their long and intimate relationship. Can. J. Neurol. Sci. 37, 313–9.

Park, C., Worth, R.M., Rubchinsky, L.L., 2011. Neural dynamics in Parkinsonian brain: The boundary between synchronized and nonsynchronized dynamics. Phys. Rev. E 83, 042901. https://doi.org/10.1103/PhysRevE.83.042901

Parthasarathy, H.B., Schall, J.D., Graybiel, A.M., 1992. Distributed but convergent ordering of corticostriatal projections: analysis of the frontal eye field and the supplementary eye field in the macaque monkey. J. Neurosci. 12, 4468–88.

Pedersen, M., Omidvarnia, A., Walz, J.M., Zalesky, A., Jackson, G.D., 2017. Spontaneous brain network activity: Analysis of its temporal complexity. Netw. Neurosci. 1, 100–115. https://doi.org/10.1162/NETN_a_00006

Pikovsky, A., Rosenblum, M., Kurths, J., 2003. phase synchronization in regular and chaotic systems. Int. J. Bifurc. Chaos 10, 2291–2305. https://doi.org/10.1142/s0218127400001481

Pizzo, F., Roehri, N., Medina Villalon, S., Trébuchon, A., Chen, S., Lagarde, S., Carron, R., Gavaret, M., Giusiano, B., McGonigal, A., Bartolomei, F., Badier, J.M., Bénar, C.G., 2019. Deep brain activities can be detected with magnetoencephalography. Nat. Commun. 10, 971. https://doi.org/10.1038/s41467-019-08665-5

Rubinov, M., Sporns, O., 2010. Complex network measures of brain connectivity: Uses and interpretations. Neuroimage 52, 1059–1069. https://doi.org/10.1016/j.neuroimage.2009.10.003

Rucco, R., Liparoti, M., Jacini, F., Baselice, F., Antenora, A., De Michele, G., Criscuolo, C., Vettoliere, A., Mandolesi, L., Sorrentino, G., Sorrentino, P., 2019. Mutations in the SPAST gene causing hereditary spastic paraplegia are related to global topological alterations in brain functional networks. Neurol. Sci. 40, 979–984. https://doi.org/10.1007/s10072-019-3725-y

Sadasivan P.K., Narayana Dutt D., 1996. SVD based technique for noise reduction in electroencephalographic signals. Signal Processing 55, 179–189.

Santangelo, G., Siciliano, M., Pedone, R., Vitale, C., Falco, F., Bisogno, R., Siano, P., Barone, P., Grossi, D., Santangelo, F., Trojano, L., 2015. Normative data for the Montreal Cognitive Assessment in an Italian population sample. Neurol. Sci. 36, 585–591. https://doi.org/10.1007/s10072-014-1995-y

Scarpetta, S., de Candia, A., 2013. Neural Avalanches at the Critical Point between Replay and Non-Replay of Spatiotemporal Patterns. PLoS One 8, e64162. https://doi.org/10.1371/journal.pone.0064162

Schulthess, I., Gorges, M., Müller, H.-P., Lulé, D., Tredici, K. Del, Ludolph, A.C., Kassubek, J., 2016. Functional connectivity changes resemble patterns of pTDP-43 pathology in amyotrophic lateral sclerosis. Nat. Publ. Gr. https://doi.org/10.1038/srep38391

Schumacher, J., Peraza, L.R., Firbank, M., Thomas, A.J., Kaiser, M., Gallagher, P., O'Brien, J.T., Blamire, A.M., Taylor, J.-P., 2019. Dysfunctional brain dynamics and their origin in Lewy body dementia. Brain. https://doi.org/10.1093/brain/awz069

Shine, J.M., Bell, P.T., Matar, E., Poldrack, R.A., Lewis, S.J.G., Halliday, G.M., O'Callaghan, C., 2019. Dopamine depletion alters macroscopic network dynamics in Parkinson's disease. Brain 142, 1024–1034. https://doi.org/10.1093/brain/awz034

Shine, J.M., Bissett, P.G., Bell, P.T., Koyejo, O., Balsters, J.H., Gorgolewski, K.J., Moodie, C.A., Poldrack, R.A., 2016. The Dynamics of Functional Brain Networks: Integrated Network States during Cognitive Task Performance. Neuron 92, 544–554. https://doi.org/10.1016/j.neuron.2016.09.018

Sorrentino, P., Nieboer, D., Twisk, J.W.R., Stam, C.J., Douw, L., Hillebrand, A., 2017. The Hierarchy of Brain Networks Is Related to Insulin Growth Factor-1 in a Large, Middle-Aged, Healthy Cohort: An Exploratory Magnetoencephalography Study. Brain Connect. 7. https://doi.org/10.1089/brain.2016.0469

Sorrentino, P., Rucco, R., Jacini, F., Trojsi, F., Lardone, A., Baselice, F., Femiano, C., Santangelo, G., Granata, C., Vettoliere, A., Monsurrò, M.R., Tedeschi, G., Sorrentino, G., 2018. Brain functional networks become more connected as amyotrophic lateral sclerosis progresses: a source level magnetoencephalographic study. NeuroImage Clin. 20, 564–571. https://doi.org/10.1016/j.nicl.2018.08.001

Spillantini, M.G., Crowther, R.A., Jakes, R., Hasegawa, M., Goedert, M., 1998. Synuclein in filamentous inclusions of Lewy bodies from Parkinson's disease and dementia with Lewy bodies (ubiquitinsarkosyl-insoluble filamentsimmunoelectron microscopy), Neurobiology Communicated by Max F. Perutz, Medical Research Council.

Sporns, O., Tononi, G., Kötter, R., 2005. The Human Connectome: A Structural Description of the Human Brain. PLoS Comput. Biol. 1, e42. https://doi.org/10.1371/journal.pcbi.0010042

Stewart, C. V, Plenz, D., 2006. Inverted-U profile of dopamine-NMDA-mediated spontaneous avalanche recurrence in superficial layers of rat prefrontal cortex. J. Neurosci. 26, 8148–59. https://doi.org/10.1523/JNEUROSCI.0723-06.2006

Stoffers, D., Bosboom, J.L.W., Deijen, J.B., Wolters, E.C., Stam, C.J., Berendse, H.W., 2008. Increased cortico-cortical functional connectivity in early-stage Parkinson's disease: An MEG study. Neuroimage 41, 212–222. https://doi.org/10.1016/J.NEUROIMAGE.2008.02.027

Sunwoo, M.K., Cha, J., Ham, J.H., Song, S.K., Hong, J.Y., Lee, J.-M., Sohn, Y.H., Lee, P.H., 2015. Olfactory performance and resting state functional connectivity in non-demented drug naïve patients with Parkinson's disease. Hum. Brain Mapp. 36, 1716–27. https://doi.org/10.1002/hbm.22732

Szewczyk-Krolikowski, K., Menke, R.A.L., Rolinski, M., Duff, E., Salimi-Khorshidi, G., Filippini, N., Zamboni, G., Hu, M.T.M., Mackay, C.E., 2014. Functional connectivity in the basal ganglia network differentiates PD patients from controls. Neurology 83, 208–14. https://doi.org/10.1212/WNL.0000000000000592

Tagliazucchi, E., Carhart-Harris, R., Leech, R., Nutt, D., Chialvo, D.R., 2014. Enhanced repertoire of brain dynamical states during the psychedelic experience. Hum. Brain Mapp. 35, 5442–56. https://doi.org/10.1002/hbm.22562

Tessitore, A., Amboni, M., Esposito, F., Russo, A., Picillo, M., Marcuccio, L., Pellecchia, M.T., Vitale, C., Cirillo, M., Tedeschi, G., Barone, P., 2012. Resting-state brain connectivity in patients with Parkinson's disease and freezing of gait. Parkinsonism Relat. Disord. 18, 781–787. https://doi.org/10.1016/j.parkreldis.2012.03.018

Tomlinson, C.L., Stowe, R., Patel, S., Rick, C., Gray, R., Clarke, C.E., 2010. Systematic review of levodopa dose equivalency reporting in Parkinson's disease. Mov. Disord. 25, 2649–2653. https://doi.org/10.1002/mds.23429

Tzourio-Mazoyer, N., Landeau, B., Papathanassiou, D., Crivello, F., Etard, O., Delcroix, N., Mazoyer, B., Joliot, M., 2002. Automated anatomical labeling of activations in SPM using a macroscopic anatomical parcellation of the MNI MRI single-subject brain. Neuroimage 15, 273–89. https://doi.org/10.1006/nimg.2001.0978

Van Veen, B.D., Van Drongelen, W., Yuchtman, M., Suzuki, A., 1997. Localization of Brain Electrical Activity via Linearly Constrained Minimum Variance Spatial Filtering. IEEE Trans. Biomed. Eng. 44.

Wei, W., Rubin, J.E., Wang, X.-J., 2015. Role of the indirect pathway of the basal ganglia in perceptual decision making. J. Neurosci. 35, 4052–64. https://doi.org/10.1523/JNEUROSCI.3611-14.2015

Weingarten, C.P., Sundman, M.H., Hickey, P., Chen, N., 2015. Neuroimaging of Parkinson's disease: Expanding

views. Neurosci. Biobehav. Rev. 59, 16–52. https://doi.org/10.1016/j.neubiorev.2015.09.007

Wiesman, A.I., Heinrichs-Graham, E.C., McDermott, T.J., Santamaria, P.M., Gendelman, H.E., Wilson, T.W., 2016. Quiet connections: Reduced fronto-temporal connectivity in nondemented Parkinson's Disease during working memory encoding. Hum. Brain Mapp. 37, 3224–3235. https://doi.org/10.1002/HBM.23237

Yang, H., Shew, W.L., Roy, R., Plenz, D., 2012. Maximal Variability of Phase Synchrony in Cortical Networks with Neuronal Avalanches. J. Neurosci. 32, 1061–1072. https://doi.org/10.1523/JNEUROSCI.2771-11.2012

Zalesky, A., Fornito, A., Cocchi, L., Gollo, L.L., Breakspear, M., 2014. Time-resolved resting-state brain networks. Proc. Natl. Acad. Sci. U. S. A. 111, 10341–6. https://doi.org/10.1073/pnas.1400181111

Zesiewicz, T.A., Sullivan, K.L., Hauser, R.A., 2006. Nonmotor symptoms of Parkinson's disease. Expert Rev. Neurother. 6, 1811–1822. https://doi.org/10.1586/14737175.6.12.1811

Zhang, Y., Wu, I.-W., Buckley, S., Coffey, C.S., Foster, E., Mendick, S., Seibyl, J., Schuff, N., 2015. Diffusion tensor imaging of the nigrostriatal fibers in Parkinson's disease. Mov. Disord. 30, 1229–1236. https://doi.org/10.1002/mds.26251

Supplementary Figures

Supplementary figure 1. Differences in the size of functional repertoire in Parkinson patients (PD) and healthy controls (HC) with different binnings. On the top, no binning (binning = 1). On the bottom, binning =5.

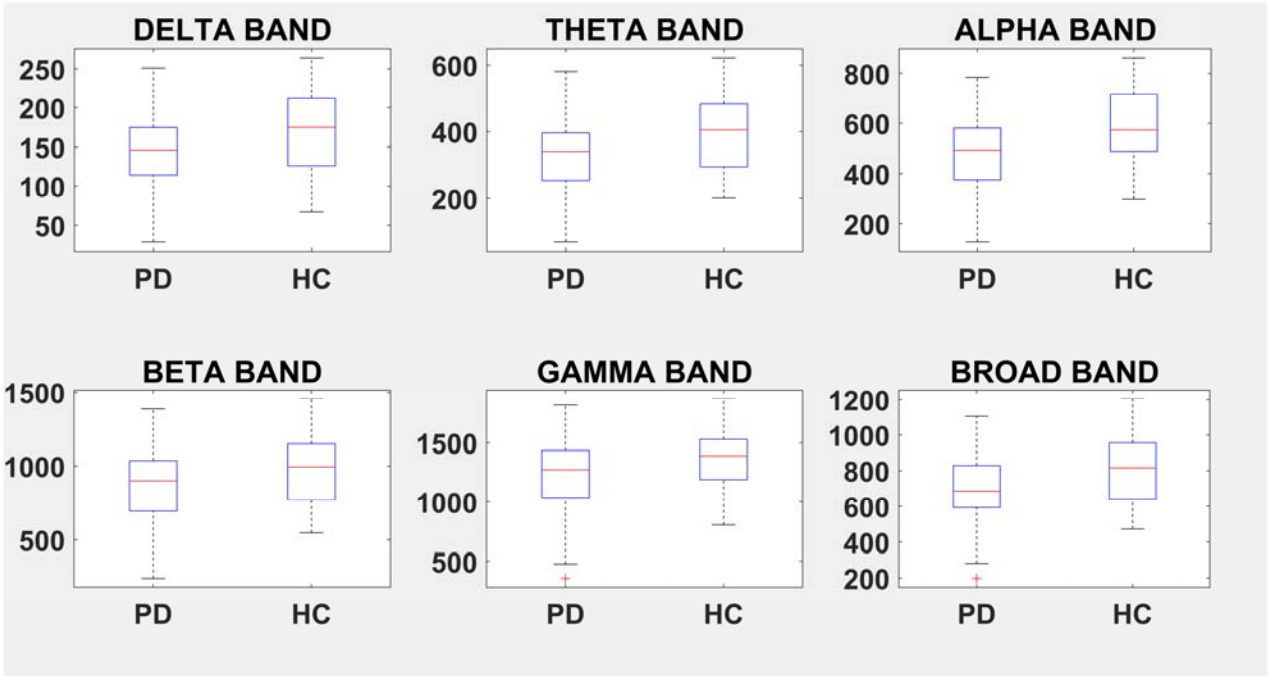

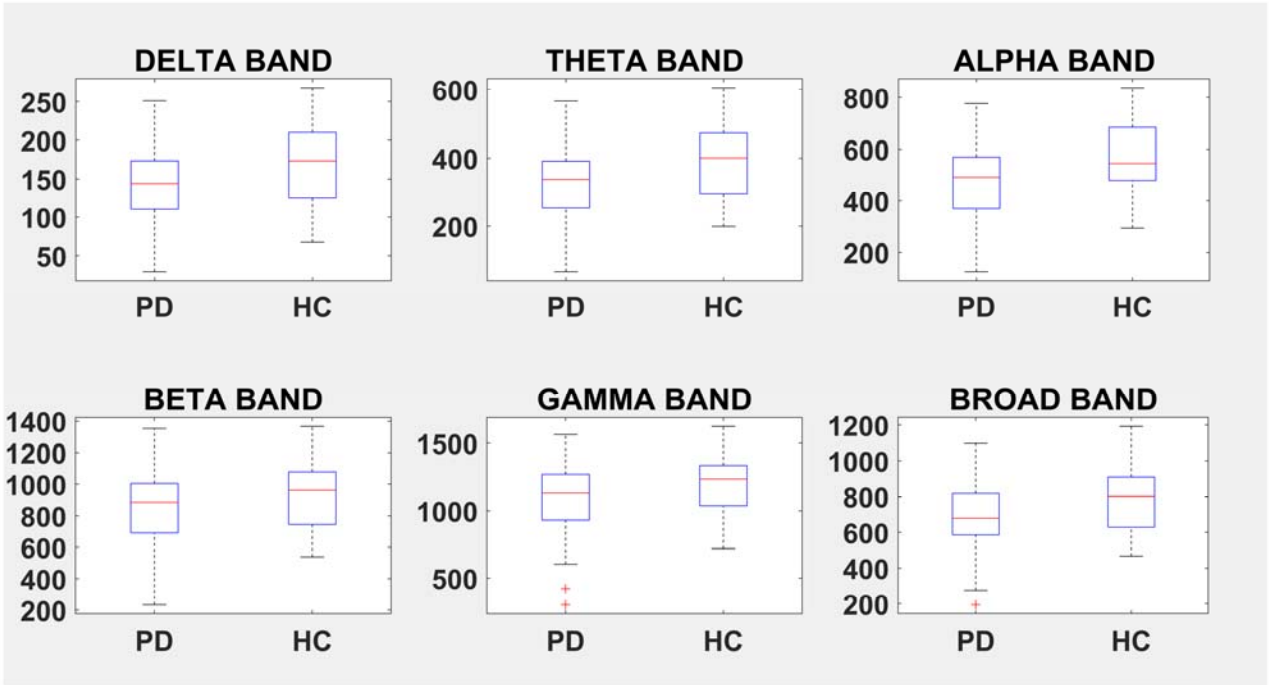

Supplementary figure 2. Differences in the size of the functional repertoire in Parkinson patients (PD) and healthy controls (HC) with different thresholds. On the top, threshold = 2.5. On the bottom, threshold = 3.5.

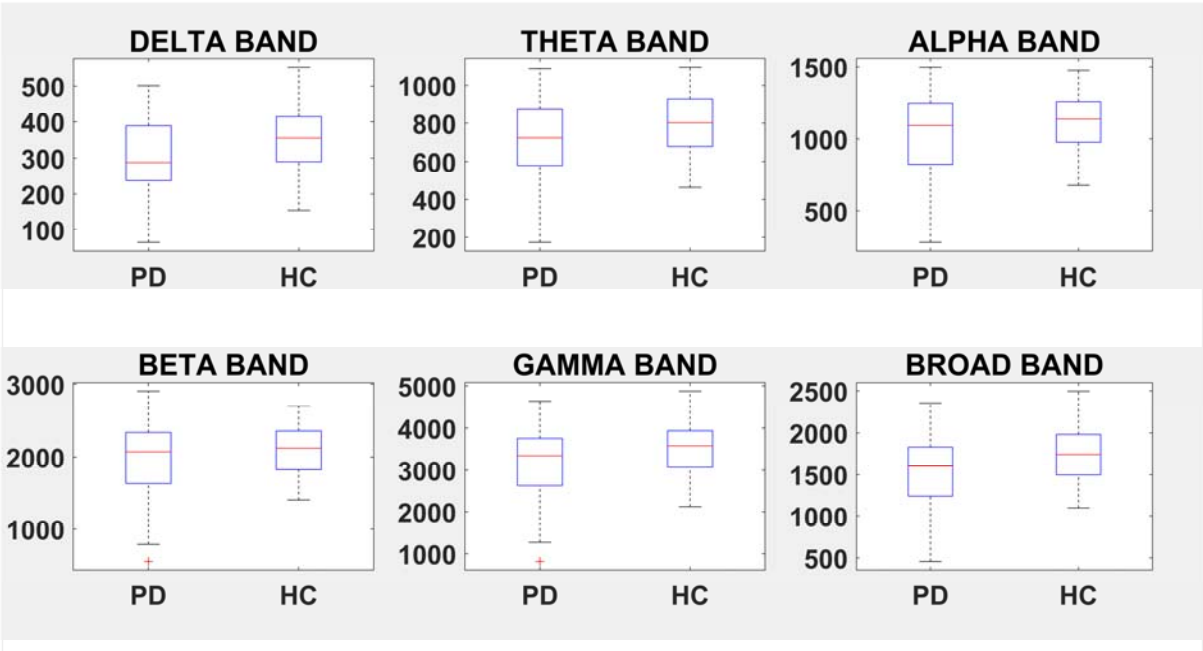

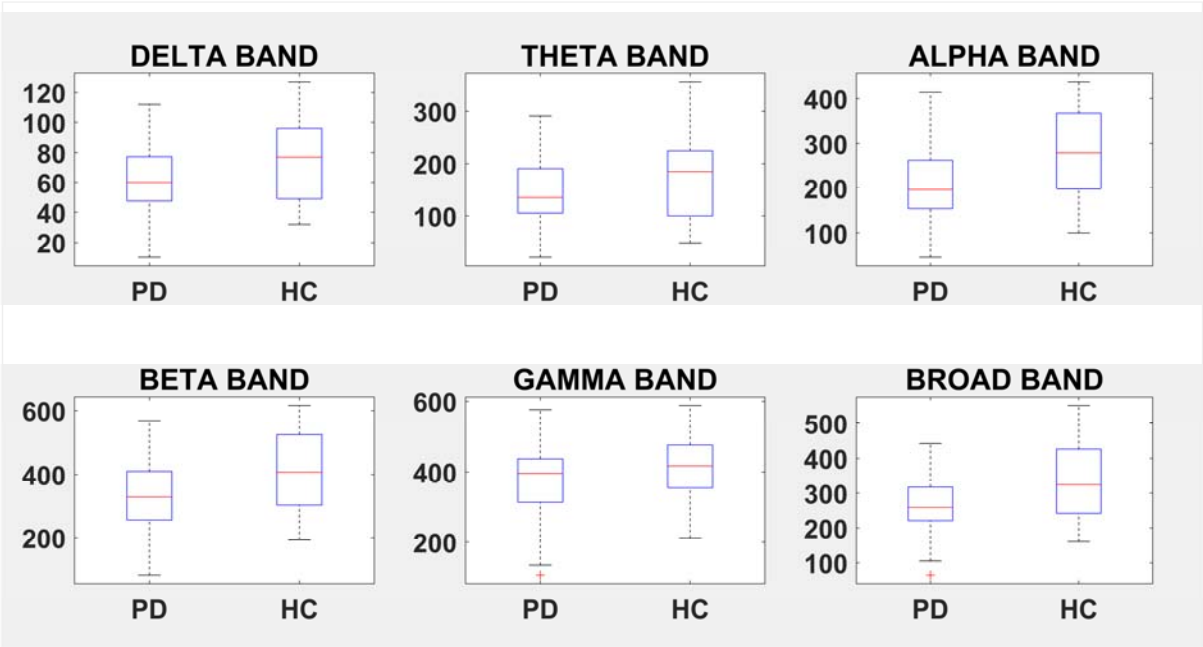

Supplementary figure 3. Differences in the size of the functional repertoire in Parkinson patients (PD) and healthy controls (HC), taking into account 90 brain areas (top) and 116 brain areas (bottom).

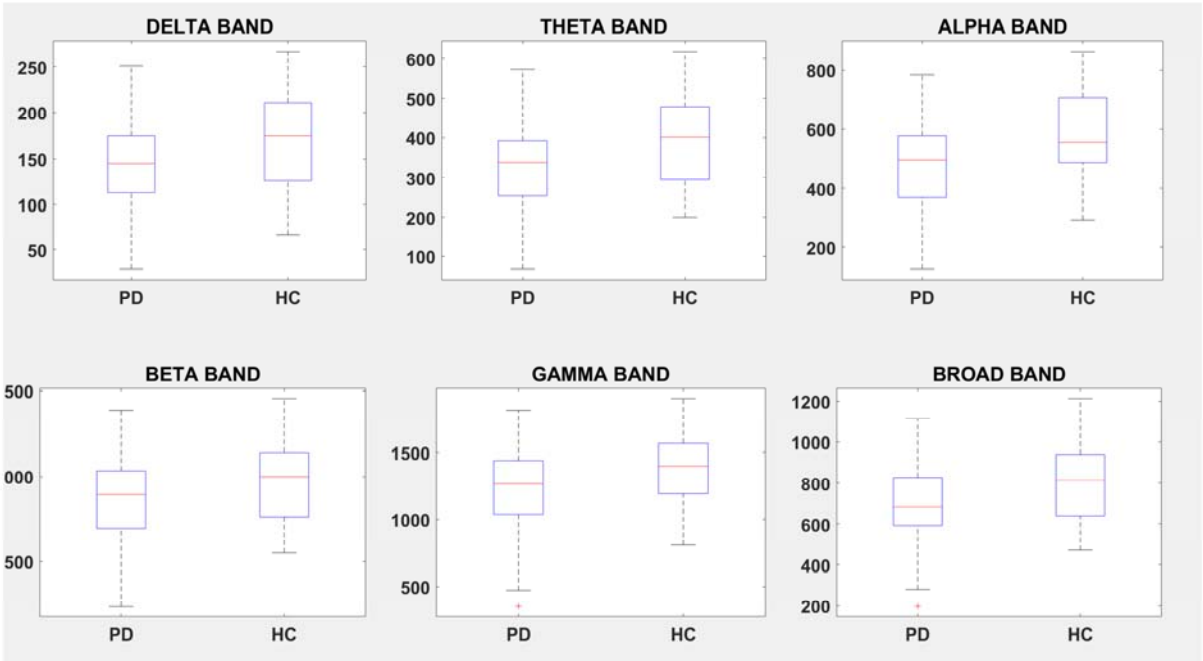

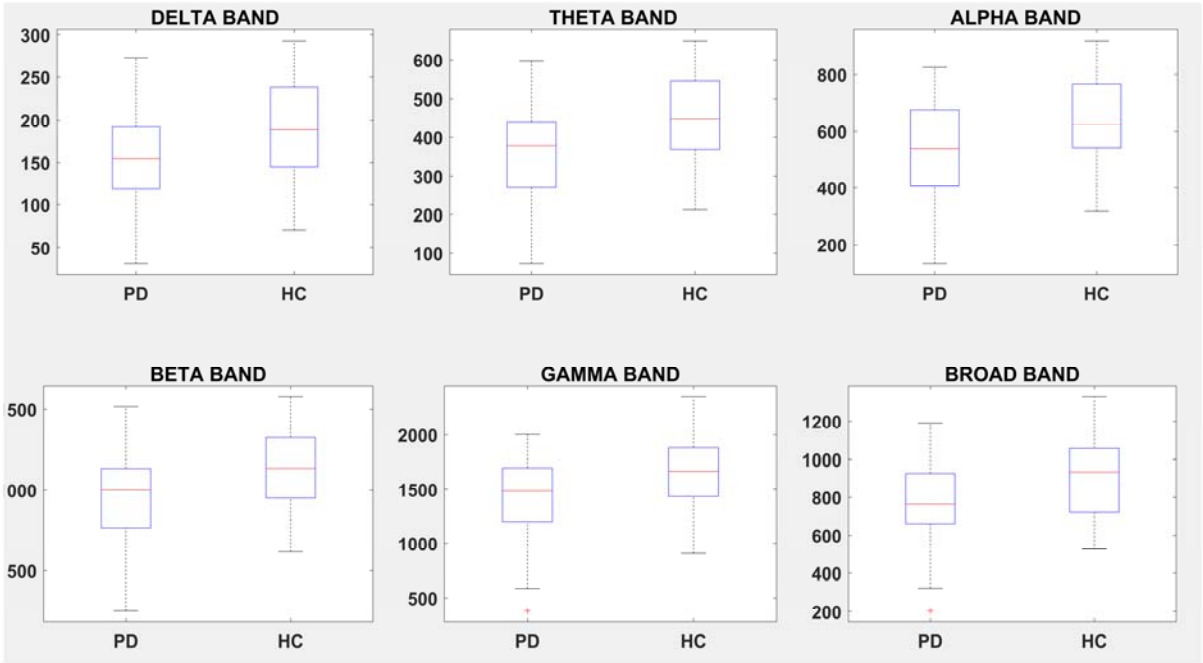
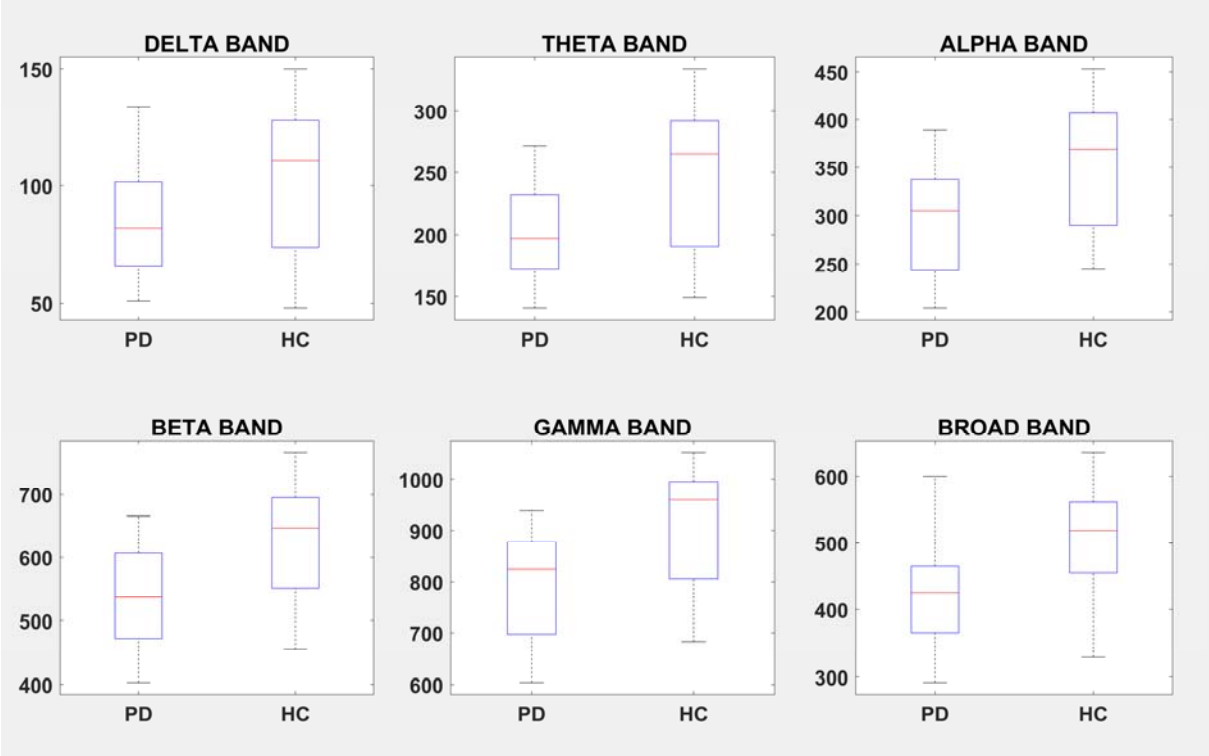
Supplementary figure 4. Differences in the size of the functional repertoire in Parkinson patients (PD) and healthy controls (HC), with the same length of data for each participant.